Chemical Engineering Communications

ISSN: 0098-6445 (Print) 1563-5201 (Online) Journal homepage: http://www.tandfonline.com/loi/gcec20

Biosorption of silver from aqueous solutions using wine industry wastes

Leticia B. Escudero, Gabriel Vanni, Fábio A. Duarte, Tássia Segger & Guilherme L. Dotto

To cite this article: Leticia B. Escudero, Gabriel Vanni, Fábio A. Duarte, Tássia Segger & Guilherme L. Dotto (2018) Biosorption of silver from aqueous solutions using wine industry wastes, Chemical Engineering Communications, 205:3, 325-337, DOI: 10.1080/00986445.2017.1387856

To link to this article: https://doi.org/10.1080/00986445.2017.1387856

Accepted author version posted online: 20 Oct 2017.
Published online: 10 Jan 2018.

CHEMICAL ENGINEERING COMMUNICATIONS
2018, VOL. 205, NO. 3, 325–337
https://doi.org/10.1080/00986445.2017.1387856

Taylor & Francis
Taylor & Francis Group

Biosorption of silver from aqueous solutions using wine industry wastes

Leticia B. Escudero[a], Gabriel Vanni[b], Fábio A. Duarte[c], Tássia Segger[c], and Guilherme L. Dotto[b]

[a]Laboratory of Analytical Chemistry for Research and Development (QUIANID), Facultad de Ciencias Exactas y Naturales, Universidad Nacional de Cuyo, Mendoza, Argentina; [b]Department of Chemical Engineering, Federal University of Santa Maria (UFSM), Santa Maria, RS, Brazil; [c]Department of Chemistry, Federal University of Santa Maria (UFSM), Santa Maria, RS, Brazil

ABSTRACT

The potential of wine industry wastes (grape peel, seed, and stem) as alternative biosorbents to remove Ag from aqueous media was investigated in this work. Wine industry wastes were washed, lyophilized and pulverized to obtain the biosorbents. The powdered biosorbents were characterized in detail and several batch experiments were performed to found the most suitable conditions for Ag biosorption. Kinetic, equilibrium, and thermodynamic studies were also performed. The interactions Ag-biosorbent were elucidated by analyses before and after the biosorption. For all wastes, the maximum removal percentages were found using a biosorbent dosage of 3.0 g L^{-1} at pH of 7.0. The kinetic data were well represented by the pseudo-first-order model. The equilibrium was satisfactorily represented by the Sips model. The maximum biosorption capacities, found at 298 K, were: 41.7, 61.4, and 46.4 mg g^{-1} for grape peel, seed, and stem, respectively. Thermodynamically, the biosorption was a spontaneous, favorable, exothermic, and enthalpy-controlled process. The magnitude of ΔH^0 indicated a physical sorption. These results showed that the wine industry wastes can be considered alternative efficient, low-cost, and eco-friendly biosorbents to remove Ag from aqueous media.

KEYWORDS

Biosorption; eco-friendly biosorbent; grape; silver; wine wastes

Introduction

Silver (Ag) is a precious metal which has been used in several industries, such as photographic, electroplating, batteries, and some others (Sari and Tüzen, 2013). As a result of these activities, amounts of Ag are released into the effluents of these industries (Wajima, 2016). It is estimated that around 6% of the Ag present in industrial effluents is directly released into the environment (Muñoz et al., 2017). According to the World Health Organization and the US Environmental Protection Agency, soluble Ag ions are classified as hazardous substances in aqueous media. In addition to the environmental aspects, the economic aspects are also important in this case, since Ag is a precious metal and should be recovered for reuse purposes. In this sense, the removal-recovery of Ag from aqueous media is a first-order concern (Tappin et al., 2010; Cantuaria et al., 2016).

Different operations have been used to remove Ag from aqueous media, like separation membrane, chemical precipitation, ion exchange, oxidation, adsorption, and biosorption (Wu et al., 2014; Jeon, 2015; Zhang et al., 2015; Cantuaria et al., 2016). It is clear that each operation has advantages and drawbacks. However, adsorption has gained attention in the last few years, and removal/recovery of Ag has been a very relevant topic (Jeon, 2015). Adsorption is preferred due to some characteristics, including ease of operation, low energetic requirements, and high efficiency (Franco et al., 2017; Dotto et al., 2016a). Activated carbon is the most used adsorbent, but efforts have been performed to test other materials, aiming to make the adsorption operation more attractive and cost-effective. When the adsorbent material is derived from a biomass, adsorption is named biosorption (Dotto et al., 2015). In this sense, the removal of Ag from aqueous media has been studied using macrofungus of *Pleurotus platypus* (Das et al., 2010), activated carbon nanospheres (Song et al., 2011), *Saccharomyces cerevisiae*

CONTACT Guilherme L. Dotto guilherme_dotto@yahoo.com.br Department of Chemical Engineering, Federal University of Santa Maria (UFSM), 1000 Roraima Avenue, Santa Maria 97105 900, RS, Brazil.
Color versions of one or more of the figures in the article can be found online at www.tandfonline.com/gcec.

(Chen et al., 2014), crab shell beads (Jeon, 2015), chitosan gel beads (Zhang et al., 2015), pre-treated bentonite (Cantuaria et al., 2016), and *Klebsiella* sp. 3S1 (Muñoz et al., 2017). The above studies demonstrated the importance of the search and applications of alternative and cheaper materials to remove Ag from aqueous media.

It should be highlighted that, for an effective application of biosorption, the biosorbent should contain the normal characteristics of adsorbents as well as high availability (Dotto et al., 2016b). Wine industry wastes, for example, is an available residue in the Brazil southern and also in Argentina. During the wine production, around 25% of the grape is discarded as wastes (termed "pomace" which is comprised of skins and seeds) (Dwyer et al., 2014). The management of these wastes is problematic for the industries. Otherwise, pomace contains lignin, cellulose, and hemicellulose (Yedro et al., 2015), which can be potential biosorption sites for Ag. In this way, the use of wine industry wastes as alternative biosorbents to remove Ag from aqueous solutions has a synergistic effect, contributing not only for the solid wastes management but also for the treatment of liquid effluents.

This work aimed to verify the applicability of three different wastes from wine industry, including grape peel (GPE), grape seeds (GSE), and grape stem (GST), as alternative biosorbents to remove Ag as Ag(I) from aqueous media. The wastes were obtained from a wine industry located in Mendoza (Argentina), pre-treated, and characterized according to the point of zero charge (pH_{ZPC}), Boehm titration, Fourier transform infrared spectroscopy (FTIR), scanning electron microscopy (SEM), energy X-ray dispersive spectroscopy (EDS), and X-ray mapping. For all wastes, the effects of biosorbent dosage and pH were studied. Biosorption kinetic, equilibrium, and thermodynamic studies were performed. The Ag-biosorbents interactions were also investigated.

Materials and methods

Wine industry wastes: Preparation and characterization

The wine industry wastes (peels, seeds, and stems) were collected from a wine industry located in Mendoza province, Argentina. The three materials were manually separated and processed according our previous work (Vanni et al., 2017). In brief, the materials were washed with drinking water and rinsed with Milli-Q water. Then, lyophilization (Virtis freeze mobile, model 6, USA) was performed for 48 h. The dried samples were then pulverized using a mill (Ultracomb, MO-8100A, Argentina) and sieved until the discrete particle size ranging from 80 to 110 µm. The obtained biosorbents were named GPE, GSE, and GST.

Grape peel, GSE, and GST biosorbents were characterized according to the pH_{ZPC}, Boehm titration, FTIR, SEM, EDS, and X-ray mapping. FTIR, SEM, EDS, and X-ray mapping were performed before and after the biosorption operation, aiming to confirm the biosorption mechanism. The pH_{ZPC} was obtained by the 11 points experiment (Park and Regalbuto, 1995). The acidity and basicity was verified by the Boehm titration (Goertzen et al., 2010). FTIR (Shimadzu, Prestige 21, Japan) was used to verify the functional groups of the biosorbents (Silverstein et al., 2007). The characteristics and the main elements of the biosorbents surface were assessed by SEM coupled to EDS and X-ray mapping (Jeol, JSM–6610LV, Japan) (Goldstein et al., 1992).

Biosorption assays

Batch biosorption experiments were performed to verify the effects of initial pH and biosorbent dosage on the biosorption. Initially, pH values between 1 and 8 (adjusted with 0.1 mol L^{-1} HNO_3/NaOH solutions) were evaluated, using the following conditions: initial Ag concentration of 50 mg L^{-1}, volume of solution of 50 mL, biosorbent dosage of 3.00 g L^{-1}, contact time of 4 h, agitation speed of 200 rpm at a temperature of 298 K, using a thermostated agitator (Marconi, MA 093, Brazil).

The effect of GPE, GSE, and GST dosage (from 0.25 to 3.00 g L^{-1}) was investigated under the same conditions, using the most adequate pH value defined elsewhere. At the more suitable conditions, kinetic experiments were performed. Thus, 50 mL of 25 and 50 mg L^{-1} of Ag were put in contact with 3 g L^{-1} of each biosorbent and pH was adjusted to 7.0. Then, a contact time of 4 h with an agitation speed of 200 rpm at room temperature was necessary.

The equilibrium experiments were assayed in a thermostatic agitator at 298, 308, 318, and 328 K. Erlenmeyer flasks containing 50 mL of Ag solutions with initial concentrations from 25 to 300 mg L^{-1} were prepared and the pH of each solution was also adjusted to 7.0. The flasks were placed in the thermostatic agitator to reach the suitable temperature. Then, 0.15 g of the biosorbent was added to each flask. The flasks were stirred at 200 rpm until the equilibrium.

After all the experiments, the solid phase was separated by centrifugation (Centribio, 80-2B, Brazil) at 4000 rpm for 20 min and the remaining Ag concentration in the liquid phase was measured by flame atomic absorption spectroscopy (AAS Vario 6, Analytik Jena AG). The experiments were realized in replicate ($n = 3$) using closed vessels and blanks were performed. The Ag removal percentage (%R), mass of Ag biosorbed per gram of biosorbent at any time (q_t (mg g^{-1})) and at equilibrium (q_e (mg g^{-1})) were calculated by the Eqs. (1)–(3), respectively:

$$\%R = \frac{(C_0 - C_t)}{C_0} \times 100 \quad (1)$$

$$q_t = \frac{V(C_0 - C_t)}{m} \quad (2)$$

$$q_e = \frac{V(C_0 - C_e)}{m} \quad (3)$$

Kinetic models

Information about the biosorption kinetics of Ag onto biosorbents (GPE, GSE, and GST) was found by fitting the following models: pseudo-first-order (PFO), pseudo second-order (PSO), and Elovich. The kinetic models of PFO and PSO are based on the biosorption capacity (Lagergren, 1898; Ho and McKay, 1998) The PFO model (Eq. (4)) is generally applicable over the initial 20–30 min of sorption process, while the PSO model (Eq. (5)) is suitable for the whole range of contact time.

$$q_t = q_1(1 - \exp(-k_1 t)) \quad (4)$$

$$q_t = \frac{t}{(1/k_2 q_2^2) + (t/q_2)} \quad (5)$$

The Elovich equation (Eq. (6)) is one of the most useful models for describing such activated chemical sorption and is suitable for heterogeneous systems (Liu and Liu, 2008).

$$q_t = \frac{1}{a}\ln(1 + abt) \quad (6)$$

Equilibrium models

The biosorption equilibrium curves of Ag ions on the biosorbents were modeled by the Langmuir (Eq. (7)) (Langmuir, 1918), Freundlich (Eq. (8)) (Freundlich, 1906), and Sips (Eq. (9)) (Sips, 1948) isotherms.

$$q_e = \frac{q_m k_L C_e}{1 + k_L C_e} \quad (7)$$

$$q_e = k_F C_e^{1/n} \quad (8)$$

$$q_e = \frac{q_S (k_S C_e)^{m_S}}{1 + (k_S C_e)^{m_S}} \quad (9)$$

Thermodynamic parameters

The biosorption thermodynamic parameters like Standard Gibb's free energy change (ΔG^0) (kJ mol^{-1}), standard enthalpy change (ΔH^0) (kJ mol^{-1}), and standard entropy change (ΔS^0) (kJ mol^{-1} K^{-1}) were estimated by the Eqs. (10) and (11) (Milonjic, 2007; Liu, 2009):

$$\Delta G^0 = -RT\ln(\rho_w K_D) \quad (10)$$

$$\ln(\rho_w K_D) = \frac{\Delta S^0}{R} - \frac{\Delta H^0}{RT} \quad (11)$$

where K_D is the equilibrium constant (L g^{-1}), ρ_w is the solution density (g L^{-1}), T is the temperature (K), and R is the universal gas constant (8.314 J mol^{-1} K^{-1}). The K_D values were estimated from the isotherm model that provided the best fit (Saucier et al., 2015).

Parameters estimation

The parameters of the above models (equilibrium, kinetics, and thermodynamics) were estimated by fitting of the models with the experimental data, using nonlinear regression. The quasi-Newton estimation method was used and the calculations were performed using Statistica 9.1 software (Statsoft, USA). The determination coefficient (R^2), adjusted determination coefficient (R^2_{adj}), average relative error (ARE), and sum of squared errors (SSE) were used to verify the fit quality (Dotto et al., 2013).

Results and discussion

Characteristics of grape peel, seed, and stem biosorbents

All biosorbents were initially characterized according to the pH_{ZPC}. The pH_{ZPC} values were 4.30, 6.50, and 4.45 for GPE, GSE, and GST, respectively. This shows that at pH values lower than 4.30, 6.50, and 4.45, the surface of GPE, GSE, and GST is positively charged, while it is negatively charged at pH values higher than the pH_{ZPC} of each biosorbent. The results of Boehm titrations indicated that all biosorbents were mainly acidic. Table 1 shows that the amounts of oxygenated groups (carboxylic, lactonic, and phenolic) were 20–30 times higher than the basic groups. This is in accordance with the pH_{ZPC} values.

The FTIR spectrum is performed as a qualitative analysis to determine the main functional groups that are involved in the biosorption process (Torab-Mostaedi et al., 2013). Figure 1 shows the FTIR spectra of GPE (a), GSE (b), and GST (c) before and after the biosorption process. From all figures, it is possible verify the major intense bands at 3400 cm^{-1}, which is mainly due to stretching vibration of hydroxyl groups, and at 2900 and 2800 cm^{-1}, which are assigned to C-H and CH_2 stretching vibration of aliphatic groups. In Figure 1(a), it can be also observed bands localized at 1625, 1375, and 1100 cm^{-1}, which can be attributed to alkene group (C=C stretching vibration), C-H stretching vibration of alkane groups, and C-O stretching vibration of alcohol groups, respectively. From GSE (Figure 1(b)), it can be visualized signals at 1750 (C=O stretching vibration), 1650 cm^{-1} (C=O stretching vibration), 1510 cm^{-1} (C=C stretching vibration of aromatic groups), 1400 cm^{-1} (–C–H stretching vibration of alkane groups), and the vibrational bands in the region 1300–1000 cm^{-1} that can be assigned to –CO, C–OC, and carboxylic acids. FTIR spectra of GST in Figure 1(c) shows a band at 1625 cm^{-1} (C=O stretching vibration), and at 1060 cm^{-1}, which can be are attributed to C-O stretching vibration. After the biosorption process, slight differences in the spectra can be observed, indicating that no significant chemical

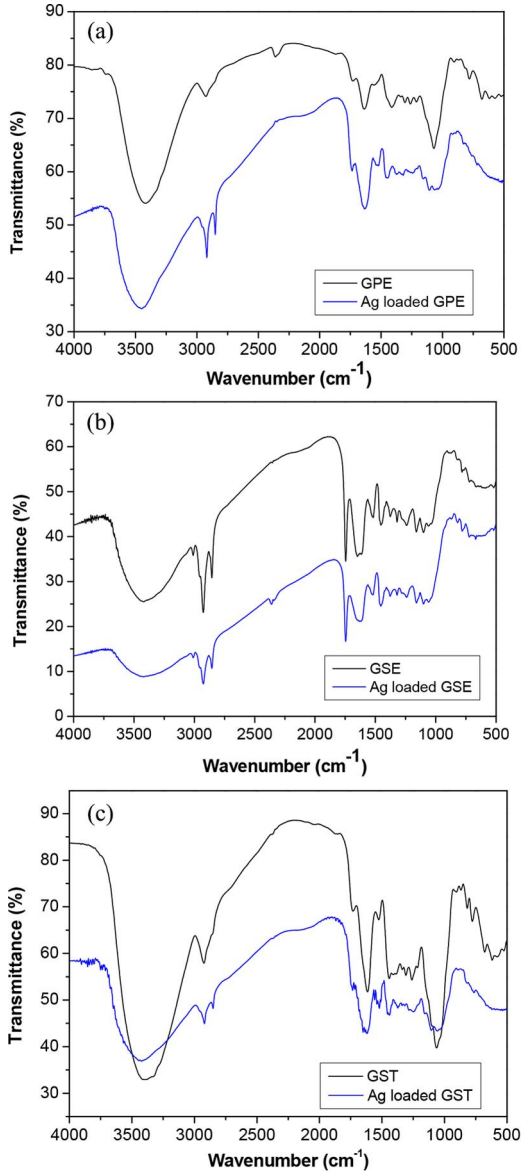

Figure 1. FTIR spectra of GPE and Ag loaded GPE (a), GSE and Ag-loaded GSE (b), and GST and Ag-loaded GST (c). *Note*: FTIR, Fourier transform infrared spectroscopy; GPE, grape peel; GSE, grape seeds; GST, grape stem.

Table 1. Surface chemistry analysis of the biosorbents by Boehm's titration.

	Acidic groups (meq g^{-1})			
Biosorbent	Carboxylic	Lactonic	Phenolic	Basic groups (meq g^{-1})
GPE	0.025 ± 0.001	0.96 ± 0.045	3.16 ± 0.13	0.08 ± 0.004
GSE	0.05 ± 0.003	0.28 ± 0.014	2.98 ± 0.14	0.01 ± 0.0005
GST	0.48 ± 0.016	0.36 ± 0.015	3.40 ± 0.13	0.16 ± 0.0075

GPE, grape peel; GSE, grape seeds; GST, grape stem.

modifications occurred during the biosorption. According to these data, we can suggest that no links were formed or broken during the biosorption process, indicating that a physical biosorption occurred.

Figure 2 shows the EDS of the three biosorbents before and after the biosorption process. Results of the EDS analysis from an average of scanned points showed that the main surface elements of GPE are C, O, and Al (Figure 2(a)). Regarding GSE, the main surface elements are C, O, Mg, P, and S (Figure 2(b)). For GST, it can be observed the presence of C, O, and Cl (Figure 2(c)). After biosorption process (Figure 2(d), (e), and (f)), the appearance of Ag can be observed, confirming the effectiveness of Ag ion biosorption onto the oenological wastes.

Scanning electron micrographs were obtained on biosorbents before and after biosorption of Ag ions (Figure 3). Regarding GPE biosorbent, it can be observed a wrinkled and uneven surface before biosorption (Figure 3(a)). After the biosorption process, it could be seen a filling and smoothing surface (Figure 3(d)). This shows that Ag ions covered the external biosorbent surface. On the other hand, the GSE reveals the presence of irregularly placed cavities before biosorption process (Figure 3(b)). After, the biosorbent reveals that the Ag ions had been densely and homogeneously adhered in the surface (Figure 3(e)). The GST biosorbent shows a heterogeneous surface with some cavities and protuberances (Figure 3(c)). After the biosorption, the GST presented the filling of some cavities and apart from that, the surface remained heterogeneous (Figure 3(f)). According to SEM, we can conclude that all the assayed biosorbents obtained good capture of Ag ions on their surfaces.

The X–ray mapping was performed after the biosorption process of Ag ions onto GPE (a), GSE (b), and GST (c) biosorbents (Figure 4). In

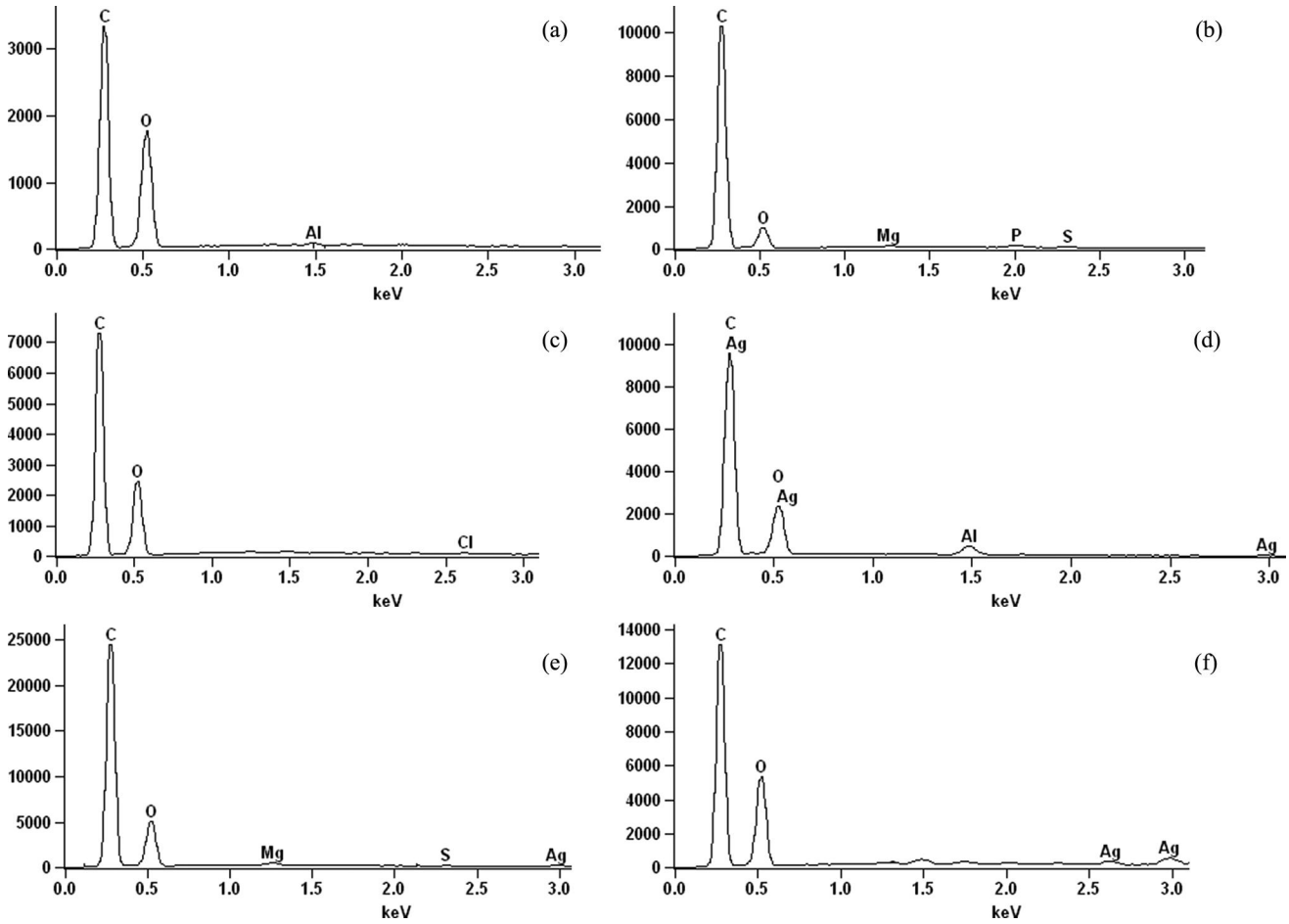

Figure 2. EDS spectra of GPE (a), GSE (b), GST (c), Ag-loaded GPE (d), Ag-loaded GSE (e), and Ag-loaded GST (f). *Note*: EDS, energy X-ray dispersive spectroscopy; GPE, grape peel; GSE, grape seeds; GST, grape stem.

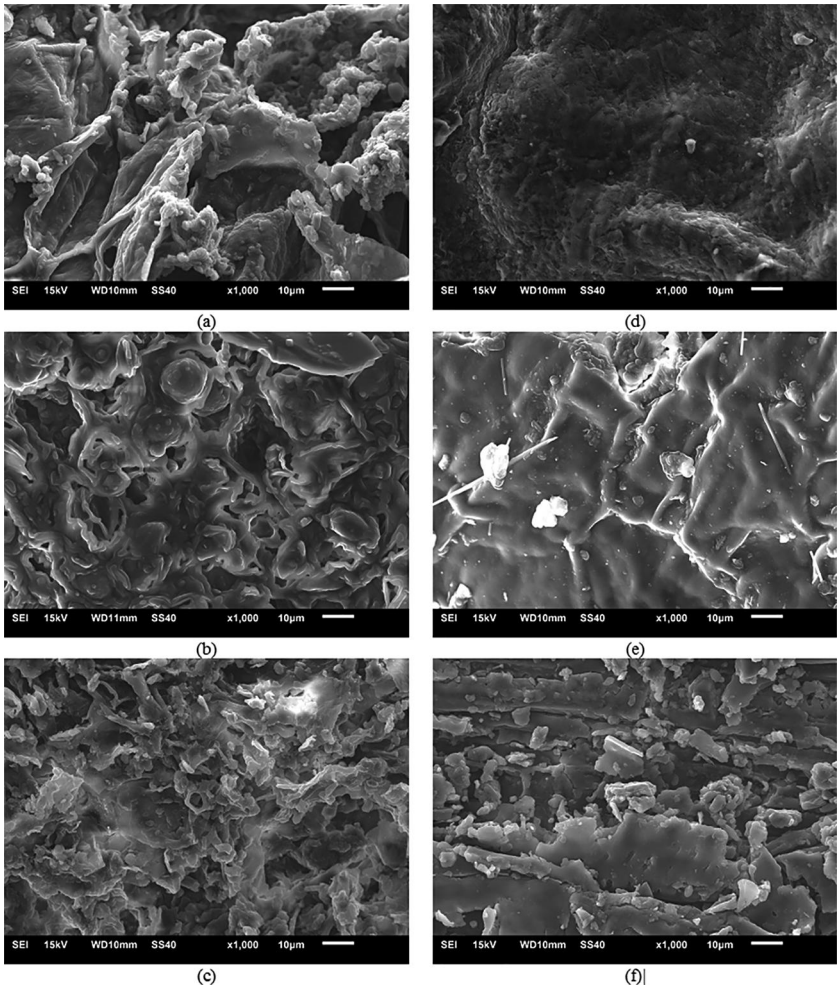

Figure 3. SEM images of GPE (a), GSE (b), GST (c), Ag-loaded GPE (d), Ag-loaded GSE (e), and Ag-loaded GST (f). *Note*: GPE, grape peel; GSE, grape seeds; GST, grape stem; SEM, scanning electron microscope.

Figure 4, the violet dots represent Ag ions. It was possible to observe a uniform distribution of Ag ions over the entire surface area of the aforementioned grape-derived materials.

Initial pH and biosorbent dosage effects

The effect of pH on biosorption of Ag ions onto GPE, GSE, and GST is shown in Figure 5(a), (b), and (c), respectively. Studies beyond pH 8 were not attempted because precipitation of the ions as hydroxides would be likely (Apiratikul and Pavasant, 2006). Figure 5(a) shows that the Ag ion removal percentage was increased at the pH from 1 to 7, reaching a maximum value at pH 7. At pH 8, it was observed a slight decrease of Ag removal. The maximum Ag ion removal percentage was almost 50%, with a biosorption capacity of GPE higher than 12 mg g^{-1}. For the GSE biosorbent, it could be observed that Ag ion removal percentage increase at the pH from 3 to 6 until it reaches maximum value at pH 7, and a slight decrease of Ag removal was also observed at higher pH values. For this biosorbent, no biosorption occurred from pH 1 and 2 while that, the Ag ion removal percentage was attained almost 50% at pH 7, with a biosorption capacity higher than 13 mg g^{-1}. Regarding GST biosorbent, the Ag ion removal percentage increases at the pH from 1 to 7, reaching Ag removal higher than 50% at pH 7, with a biosorption capacity of almost 15 mg g^{-1}. According to the pH_{ZPC} values previously reported, it can be deduced that at pH of work (pH 7.0), the surface of all biosorbents was negatively charged. In this way, the positive charges of the Ag ions could be attracted by the negatively charged surface of the biosorbents, reaching the high values of metal removal

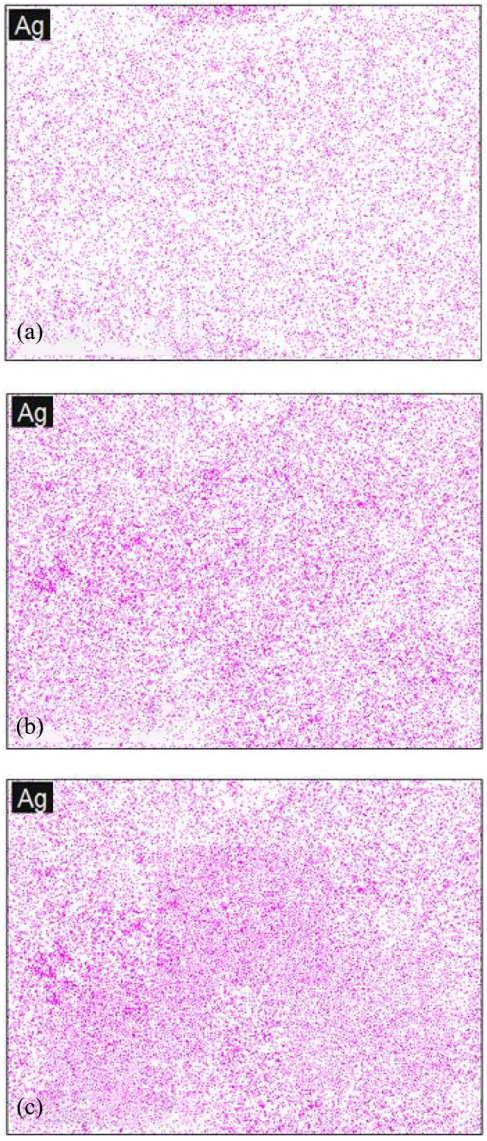

Figure 4. X–ray mappings of Ag-loaded GPE (a), Ag-loaded GSE (b), and Ag-loaded GST (c). *Note*: GPE, grape peel; GSE, grape seeds; GST, grape stem.

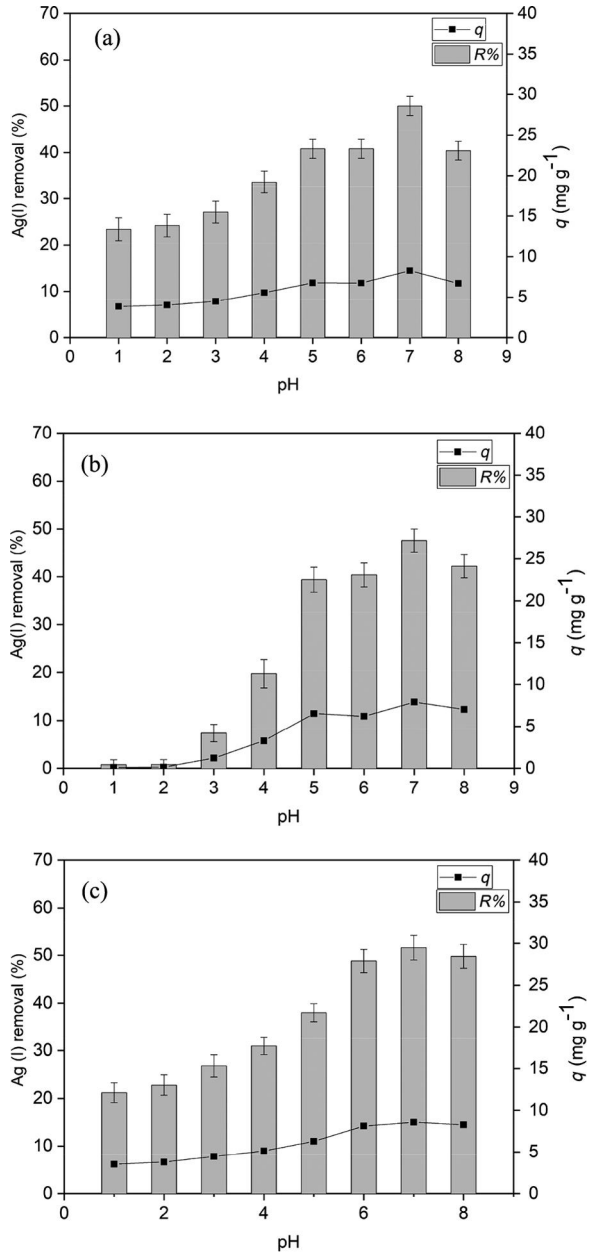

Figure 5. pH effect on the Ag(I) biosorption: GPE (a), GSE (b), and GST (c) ($C_0 = 50$ mg L^{-1}, $V = 50$ mL, biosorbent dosage of 3.00 g L^{-1}, $t = 4$ h, 200 rpm, $T = 298$ K). *Note*: GPE, grape peel; GSE, grape seeds; GST, grape stem.

percentage. This behavior can be explained by possible electrostatic interactions between the negative surface of the biosorbents and the positively charge of Ag ions. Similar trend regarding to the pH was found by Wajima (2016), studying the Ag(I) biosorption on a zeolitic material, where the best pH was 6.0. Also at pH 6.0, Jeon (2015) obtained best results for Ag(I) adsorption on immobilized crab shell beads (2.951 mg g^{-1}). In our study, pH 7.0 was selected for the subsequent studies.

The effect of biosorbent dosage is shown in Figure 6. It is possible to note that the increase in biosorbent dosage from 0.25 to 3.00 g L^{-1} caused an increase in the Ag ion removal percentage (R). However, for the biosorbent (GPE) (Figure 6(a)), the biosorption capacity (q) decreased from 49.4 to 12.7 mg g^{-1} when the biosorption dosage increased from 0.25 to 1.0 g L^{-1}, after that, the biosorption capacity had a slight decrease from 12.7 to 8.4 mg g^{-1} when the biosorbent dosage increased from 1 to 3 g L^{-1}, where it was reached a maximum value in removal percentage of 51%. For GSE biosorbent (Figure 6(b)), the increase of biosorbent dosage from 0.25 to 1.5 g L^{-1} caused an increase from 17.3 to 29.7% in the dye removal

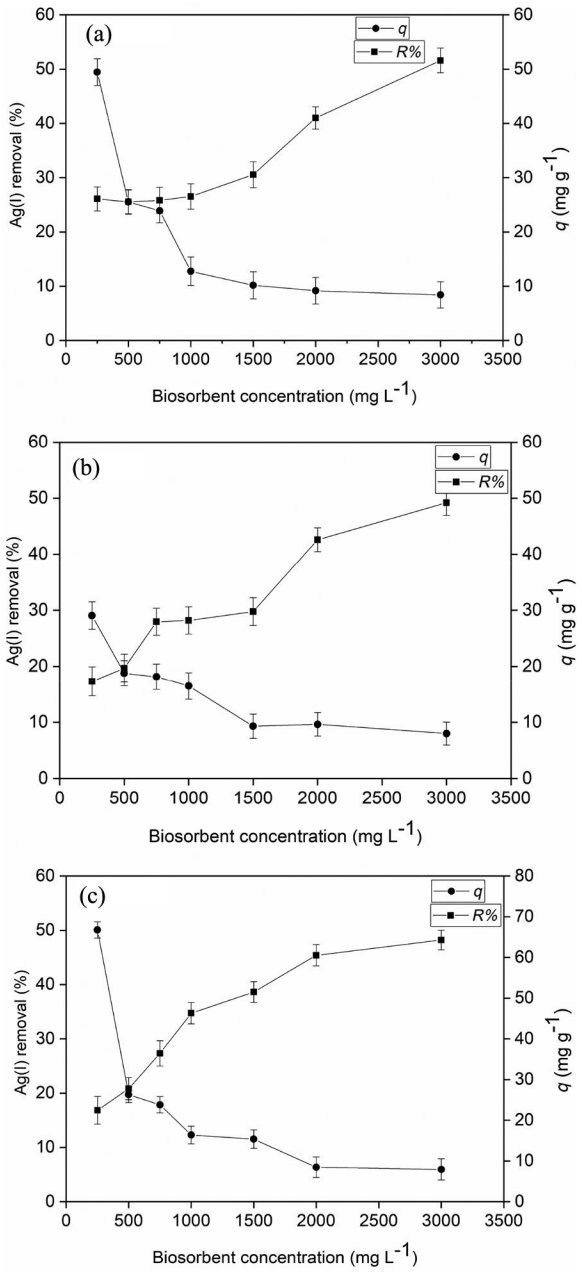

Figure 6. Biosorbent dosage effect on the Ag(I) biosorption: GPE (a), GSE (b), and GST (c) ($C_0 = 50$ mg L^{-1}, $V = 50$ mL, pH = 7.0, $t = 4$ h, 200 rpm, $T = 298$ K). *Note*: GPE, grape peel; GSE, grape seeds; GST, grape stem.

percentage (R) and the decrease from 29 to 9.3 mg g^{-1} in biosorption capacity. Nevertheless, for biosorbent dosage from 1.5 to 3 g L^{-1}, it could be observed an increase in Ag ion removal percentage, reaching a removal of Ag of 49%. For GST biosorbent (Figure 6(c)), it was observed a similar behavior than the previous biosorbents. Taking into account the previous data, the more adequate conditions for all biosorbents were pH 7.0 and biosorbent dosage of 3 g L^{-1}.

Biosorption kinetic results

Figure 7 shows the kinetic curves obtained for initial Ag ion concentrations of 25 and 50 mg L^{-1} for the three biosorbents. From GPE (Figure 7(a)), it was verified a fast uptake rate in the first stages, reaching biosorption capacities of 7 and 2 mg g^{-1}

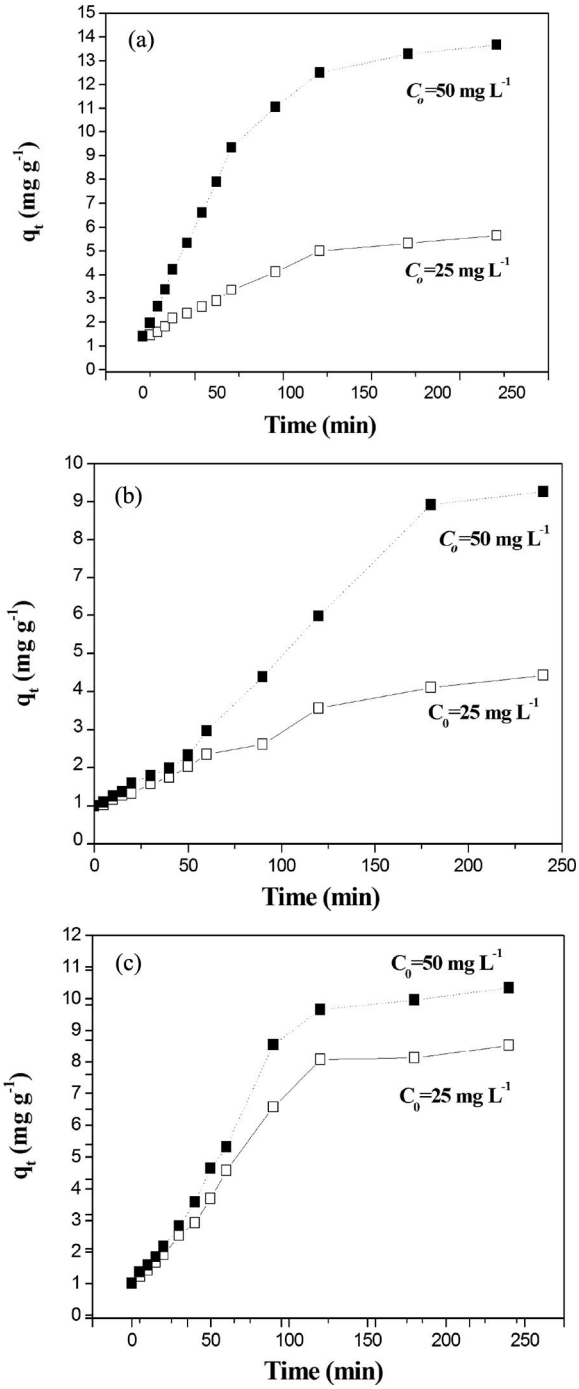

Figure 7. Kinetic curves of the Ag(I) biosorption on GPE (a), GSE (b), and GST (c) ($V = 50$ mL, pH 7.0, biosorbent dosage of 3.00 g L^{-1}, 200 rpm, $T = 298$ K). *Note*: GPE, grape peel; GSE, grape seeds; GST, grape stem.

at 120 min, for initial Ag concentrations of 50 and 25 mg L^{-1}, respectively. After this time, the biosorption rate decreased and the biosorption capacity keeps practically constant, reaching maximum values of 8.1 and 3 mg g^{-1}. For GSE biosorbent (Figure 7(b)), the curves for the two concentrations followed the same trend until the first 25 min, and then the curve of concentration of 50 mg L^{-1} continued to increase until reaches the equilibrium at 240 min, with a maximum biosorption capacity at 8.2 mg g^{-1}. Regarding GST biosorbent (Figure 7(c)), the trend is similar to the GSE biosorbent during the first 25 min, and then the curves reach almost the maximum biosorption capacities (8.6 and 6.9 mg g^{-1} for 50 and 25 mg L^{-1} of Ag, respectively).

The parameters of the kinetic models are given in Table 2. Based on the coefficient of determination ($R^2 > 0.95$) and sum of squares errors (SSE <5.2%), it can be concluded that the PFO model was the most adequate to represent the experimental data and could be used to predict the biosorption kinetic of Ag ions by the wine wastes biosorbents. Comparing the initial concentrations for each biosorbent, it can be seen that the higher values of q_1 and k_1 were found at 50 mg L^{-1}. For all biosorbents, this confirms that the higher biosorption rate and biosorption capacity were found at 50 mg L^{-1}. Comparing now the biosorbents, it was verified that GSE presented the high biosorption capacity, while GPEs presented the high biosorption rate. It is important to highlight that the experimentally determined biosorption capacities (q_{exp}) are similar to those predicted (q_1) by the PFO model.

Biosorption isotherm results

Figure 8 shows the equilibrium isotherms for the biosorption of Ag ion onto (a) GPE, (b) GSE, and (c) GST, obtained at 298, 308, 318, and 328 K. Overall, the isotherms of the three biosorbents presented the same favorable behavior, which is characterized by an initial step of increase in biosorption capacity, followed by a convex shape of the curve. All curves can be classified as type "L" normal isotherms. The initial step indicates a great biosorbents-Ag ions affinity and the convex shape suggests the saturation of the biosorption sites by the Ag ions (Giles et al., 1960). Furthermore, it can be seen for the three biosorbents that the biosorption capacity decreased with the temperature increase, indicating an exothermic process. This can be attributed to the fact that at temperatures above 318 K, some damages of sites on the biomasses surface can be occurred and, consequently a decrease in the surface activity is manifested (Aksu, 2005).

All isotherms were adjusted by Langmuir, Freundlich, and Sips models. The parameters are shown in Table 3 for all the studied temperatures. A comparison of the R^2, ARE (%), and SSE values was performed for the three models. According to data presented in Table 3, it can be observed that the Sips model showed the best adjustment for

Table 2. Kinetic parameters for the Ag(I) biosorption on GPE, GSE, and GST.

	Grape peel		Grape seeds		Grape stem	
Kinetic model	25 mg L^{-1}	50 mg L^{-1}	25 mg L^{-1}	50 mg L^{-1}	25 mg L^{-1}	50 mg L^{-1}
Pseudo-first-order						
k_1 (min^{-1})	0.007	0.013	0.004	0.005	0.008	0.008
q_1 (mg g^{-1})	3.475	8.704	5.487	12.21	2.952	10.455
R^2	0.992	0.992	0.985	0.966	0.961	0.959
SSE	0.177	0.799	0.235	3.760	0.365	5.112
Pseudo-second-order						
k_2 (g mg^{-1} min^{-1})	0.0009	0.0009	0.0004	0.0002	0.001	0.0004
q_2 (mg g^{-1})	5.297	11.856	7.888	16.55	4.566	15.226
h_0 (mg g^{-1} min^{-1})	0.025	0.126	0.003	0.036	0.020	0.092
R^2	0.990	0.984	0.983	0.959	0.955	0.951
SSE	0.223	1.654	0.280	4.574	0.428	6.124
Elovich						
a (g mg^{-1})	0.714	0.383	0.364	0.168	0.825	0.239
b (mg g^{-1} min^{-1})	0.020	0.105	0.017	0.046	0.017	0.067
R^2	0.988	0.973	0.983	0.960	0.949	0.944
SSE	0.270	2.763	0.275	4.444	0.488	6.970
q_{exp} (mg g^{-1})	2.812	8.119	3.433	8.268	6.848	8.501

GPE, grape peel; GSE, grape seeds; GST, grape stem; SSE, sum of squared errors.

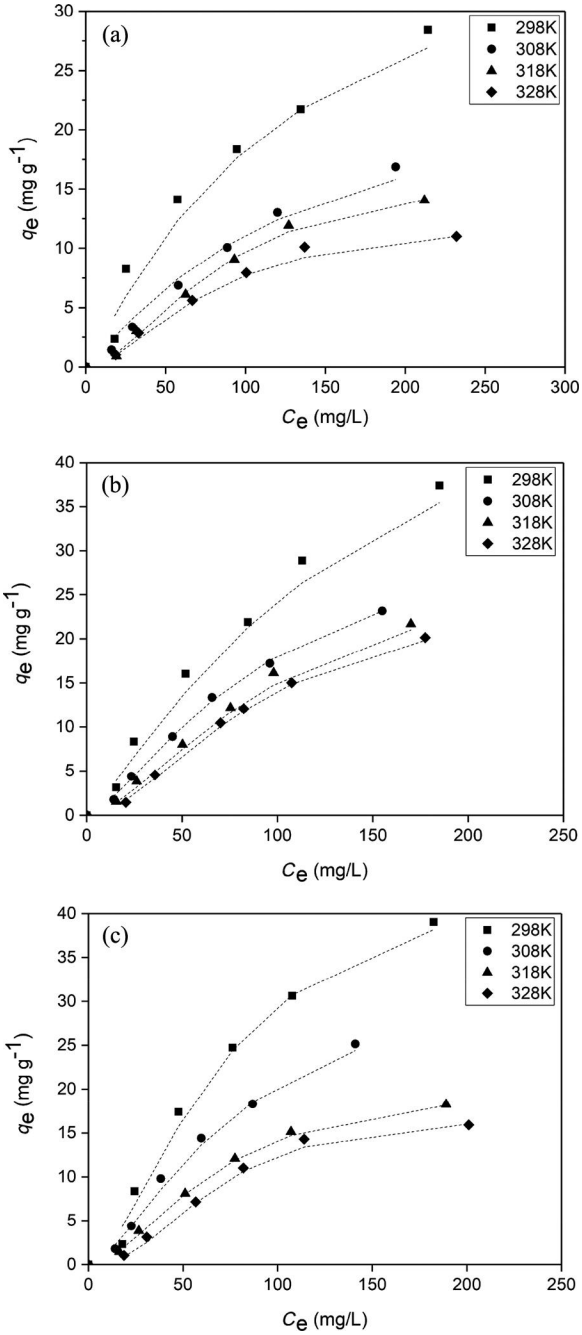

Figure 8. Isotherm curves of the Ag(I) biosorption on GPE (a), GSE (b), and GST (c) (V = 50 mL, pH 7.0, biosorbent dosage of 3.00 g L^{-1}) (Sips model, ■ 298 K, ● 308 K, ◆ 318 K, ▲ 328 K). *Note*: GPE, grape peel; GSE, grape seeds; GST, grape stem.

the three biosorbents. It is important to mention that q_S parameter decreased with the temperature, corroborating that the biosorption capacity was favored at 298 K. This behavior is attractive from the economic viewpoint, since no requirements of temperature and extra time are required for reaching the maximum biosorption capacity. The maximum biosorption capacities (q_S) reported at 298 K from the Sips model were 41.7, 61.4, and 46.4 mg g^{-1} for GPE, GSE, and GST, respectively. Jeon (2015) obtained 2.951 mg g^{-1} for Ag(I) adsorption on immobilized crab shell beads. In the study of Zhang et al. (2015), the maximum uptake of Ag by ion-imprinted chitosan beads was 89.20 mg g^{-1}. Das et al. (2010) obtained biosorption capacity of 46.7 mg g^{-1} using the macrofungus *P. platypus* as biosorbent. Song et al. (2011) obtained adsorption capacity of 152 mg g^{-1} using surface activated carbon nanospheres as Ag adsorbent. Cantuaria et al. (2016) obtained maximum adsorption capacities of 61.48 mg g^{-1} using Verde-lodo clay for Ag removal. These results indicate that the wine industry wastes (GPE, GSE, and GST) are competitive materials to uptake silver from aqueous media, in terms of biosorption capacity. Other advantages of these biosorbents are low–cost and availability. Furthermore, the use of GPE, GSE, and GST as biosorbents contributes for the solid wastes management in wine industries.

Biosorption thermodynamics

Thermodynamic parameters such as ΔG^0, ΔH^0, and ΔS^0 were calculated and are shown in Table 4. For all biosorbents, it was found that the biosorption was a spontaneous and favorable process, since the ΔG^0 values were negative. In general, more negative ΔG^0 values were found at 298 K, indicating that the biosorption was favored in this temperature. The negative values of ΔH^0 confirm that the Ag biosorption on GPE, GSE, and GST was an exothermic process. The magnitude of ΔH^0 is in agreement with physisorption (Crini and Badot, 2008). Specifically, ΔH^0 values closes with physical electrostatic interactions between the biosorbent and adsorbate, which the magnitude ranges from 20 to 80 kJ mol^{-1} (Bergmann and Machado, 2015). Comparing the values of ΔH^0 with $T\Delta S^0$, it can be seen than ΔH^0 contributes more than $T\Delta S^0$ to reach negative values of ΔG^0. This behavior shows that the Ag biosorption was an enthalpy controlled process.

Interaction mechanism

An interaction mechanism between Ag and the biosorbents was proposed on the basis in the following aspects: FTIR, pH_{ZPC}, Boehm titration,

Table 3. Isotherm parameters for the Ag(I) biosorption on GPE, GSE, and GST.

	Grape peel				Grape seeds				Grape stem			
Isotherm model	298 K	308 K	318 K	328 K	298 K	308 K	318 K	328 K	298 K	308 K	318 K	328 K
					Langmuir							
q_m (mg g^{-1})	48.5	45.8	32.5	20.1	87.0	67.9	71.5	67.7	82.8	76.4	36.9	33.8
k_L (L mg^{-1})	0.006	0.003	0.003	0.005	0.004	0.003	0.002	0.002	0.005	0.003	0.005	0.005
R^2	0.982	0.994	0.976	0.974	0.994	0.992	0.987	0.982	0.978	0.986	0.977	0.951
R^2_{adj}	0.978	0.992	0.971	0.968	0.992	0.990	0.984	0.978	0.973	0.983	0.972	0.941
ARE (%)	20.70	10.059	26.58	19.63	11.49	14.81	17.53	23.34	32.68	21.53	23.03	38.10
SSE	11.17	1.25	4.14	2.96	6.66	3.37	4.74	5.66	27.92	6.85	6.58	11.99
					Freundlich							
k_F ((mg g^{-1}) (mg L^{-1})$^{-1/nF}$)	0.938	0.275	0.278	0.367	0.796	0.402	0.307	0.269	0.962	0.442	0.512	0.405
$1/n$	1.56	1.267	1.34	1.55	1.345	1.232	1.193	1.187	1.384	1.213	0.696	1.405
R^2	0.972	0.986	0.957	0.943	0.985	0.984	0.979	0.973	0.960	0.978	0.953	0.921
R^2_{adj}	0.966	0.983	0.948	0.931	0.982	0.980	0.974	0.967	0.952	0.973	0.943	0.905
ARE (%)	26.43	15.51	32.34	27.80	16.48	18.90	20.79	26.53	40.36	25.55	30.35	44.26
SSE	0.61	3.23	1.26	1.30	15.93	6.87	7.99	8.71	52.10	11.19	13.78	19.40
					Sips							
q_S (mg g^{-1})	41.7	25.4	16.8	12.6	61.4	33.8	30.0	25.9	46.4	33.9	21.0	17.3
k_S (L mg^{-1})	0.008	0.008	0.012	0.013	0.007	0.011	0.010	0.011	0.014	0.013	0.015	0.015
m_S	1.115	1.138	1.779	1.753	1.206	1.454	1.598	1.770	1.638	1.555	1.787	2.297
R^2	0.983	0.999	0.996	0.995	0.995	0.998	0.998	0.999	0.993	0.996	0.999	0.997
R^2_{adj}	0.974	0.998	0.994	0.992	0.992	0.997	0.997	0.998	0.997	0.994	0.998	0.995
ARE (%)	19.4	2.14	7.46	4.40	8.89	4.60	3.16	4.59	17.57	8.04	3.63	3.81
SSE	10.7	0.08	0.58	0.55	4.64	0.43	0.49	0.22	8.57	1.89	0.20	0.65

ARE, average relative error; GPE, grape peel; GSE, grape seeds; GST, grape stem; SSE, sum of squared errors.

Table 4. Thermodynamic parameters for the Ag(I) biosorption on GPE, GSE, and GST.

	ΔG^0 (kJ mol^{-1})			ΔH^0 (kJ mol^{-1})			ΔS^0 (kJ mol^{-1} K^{-1})		
T (K)	GPE	GSE	GST	GPE	GSE	GST	GPE	GSE	GST
298	−14.38	−15.00	−16.03	−17.85	−25.48	−28.60	−0.01	0.01	−0.03
308	−13.58	−15.13	−15.56						
318	−13.99	−15.04	−15.17						
328	−13.85	−15.36	−15.11						

GPE, grape peel; GSE, grape seeds; GST, grape stem.

Ag speciation, pH effect and thermodynamic results. At pH of 7.0, the biosorbents are negatively charged, since the pH_{ZPC} values were 4.30, 6.50, and 4.45 for GPE, GSE, and GST, respectively. In parallel, Ag is monovalent cationic specie in the form of Ag^+. Then, electrostatic interaction between the acidic groups contained in the biosorbents surface and the Ag^+ explains the biosorption. This interaction mechanism is corroborated by the FTIR study, which reveals that no links were formed or broken during the biosorption process, indicating that a physical biosorption occurred. Also, the ΔH^0 values closed with physical electrostatic interactions between the biosorbent and adsorbate.

Conclusion

This work demonstrates the potential of wine industry wastes (grape peel, seed, and stem) as biosorbents to remove Ag from aqueous solutions, to contribute with the solid wastes management in wine industries. It was found that the wine industry wastes contain acidic character and pH_{ZPC} lower than 6.5, being more adequate to uptake cationic species. The more adequate conditions for Ag biosorption were pH 7.0 and biosorbent dosage of 3 g L^{-1}. The biosorption kinetic profile can be represented by the PFO model. The Sips model was suitable to represent the biosorption isotherms, being the maximum biosorption capacities of 41.7, 61.4, and 46.4 mg g^{-1} for grape peel, seed, and stem, respectively; obtained at 298 K. Biosorption was spontaneous, favorable and exothermic. It is reasonable infer that electrostatic interactions between the negatively charged surface of the wine wastes and Ag^+ was the main biosorption interaction mechanism. These results show that a possible application for the wine industry wastes,

to contribute with the solid wastes management in the wine industries, is the Ag(I) uptake from aqueous media.

Funding

The authors would like to thank National Council for Scientific and Technological Development (CNPq), Consejo Nacional de Investigaciones Científicas y Técnicas (CONICET), Agencia Nacional de Promoción Científica y Tecnológica (FONCYT) (Project PICT-2015-1338), and Universidad Nacional de Cuyo for the financial support.

Nomenclature

$1/n$	heterogeneity factor
$\%R$	Ag removal percentage (%)
a	desorption constant of the Elovich model (g mg^{-1})
ARE	average relative error (%)
b	initial velocity due to dq/dt with $q_t = 0$ (mg g^{-1} min^{-1})
C_0	initial Ag concentration in liquid phase (mg L^{-1})
C_t	Ag concentration in liquid phase at any time (mg L^{-1})
C_e	equilibrium Ag concentration in liquid phase (mg L^{-1})
EDS	energy X-ray dispersive spectroscopy
FTIR	Fourier transform infrared spectroscopy
GPE	grape peel
GSE	grape seeds
GST	grape stem
k_1	pseudo-first-order kinetic constant (min^{-1})
k_2	pseudo-second-order kinetic constant (g mg^{-1} min^{-1})
K_D	equilibrium constant (L g^{-1})
k_F	Freundlich constant (mg g^{-1}) (mg L^{-1})$^{-1/n}$
k_L	Langmuir constant (L mg^{-1})
k_S	Sips constant (L mg^{-1})
m	mass of biosorbent (g)
m_S	Sips exponent
PFO	pseudo-first-order
PSO	pseudo-second-order
pH_{ZPC}	point of zero charge
q_1	biosorption capacity from the pseudo-first-order model (mg g^{-1})
q_2	biosorption capacity from the pseudo-second-order model (mg g^{-1})
q_t	mass of Ag biosorbed per gram of biosorbent at any time (mg g^{-1})
q_e	mass of Ag biosorbed at equilibrium (mg g^{-1})
q_m	maximum biosorption capacity from Langmuir model (mg g^{-1})
q_S	maximum biosorption capacity from Sips model (mg g^{-1})
R	universal gas constant (J mol^{-1} K^{-1})
R^2	coefficient of determination
R^2_{adj}	adjusted determination coefficient
SEM	scanning electron microscopy
SSE	sum of squared error (mg^2 g^{-2})
t	time (min)
T	temperature (K)
V	volume of solution (L)

Greek symbols

ΔG^0	standard Gibbs free energy change (kJ mol^{-1})
ΔH^0	standard enthalpy change (kJ mol^{-1})
ΔS^0	standard entropy change (kJ mol^{-1} K^{-1})
ρ_w	solution density (g L^{-1})

References

Apiratikul, R., and Pavasant, P. (2006). Sorption isotherm model for binary component sorption of copper, cadmium, and lead ions using dried green macroalga *Caulerpa lentillifera*, *Chem. Eng. J.*, **119**, 135–145.

Aksu, Z. (2005). Application of biosorption for the removal of organic pollutants: A review, *Proc. Biochem.*, **40**, 997–1026.

Bergmann, C. P., and Machado, F. M. (2015). *Carbon Nanomaterials as Adsorbents for Environmental and Biological Applications*, Springer Cham, Heidelberg, New York.

Cantuaria, M. L., Almeida Neto, A. F., Nascimento, E. S., and Vieira, M. G. A. (2016). Adsorption of silver from aqueous solution onto pre–treated bentonite clay: Complete batch system evaluation, *J. Clean. Prod.*, **112**, 1112–1121.

Chen, C., Wen, D., and Wang, J. (2014). Cellular surface characteristics of *Saccharomyces cerevisiae* before and after Ag(I) biosorption, *Bioresour. Technol.*, **156**, 380–383.

Crini, G., and Badot, P. M. (2008). Application of chitosan, a natural aminopolysaccharide, for dye removal from aqueous solutions by adsorption processes using batch studies: A review of recent literature, *Prog. Polym. Sci.*, **33**, 399–447.

Das, D., Das, N., and Mathew, L. (2010). Kinetics, equilibrium and thermodynamic studies on biosorption of Ag(I) from aqueous solution by macrofungus *Pleurotus platypus*, *J. Hazard. Mater.*, **184**, 765–774.

Dotto, G. L., Costa, J. A. V., and Pinto, L. A. A. (2013). Kinetic studies on the biosorption of phenol by nanoparticles from Spirulina sp. LEB 18, *J. Environ. Chem. Eng.*, **1**, 1137–1143.

Dotto, G. L., Meili, L., Souza Abud, A. K., Tanabe, E. H., Bertuol, D. A., and Foletto, E. L. (2016a). Comparison between Brazilian agro-wastes and activated carbon as adsorbents to remove Ni(II) from aqueous solutions, *Water Sci. Technol.*, **73**, 2713–2721.

Dotto, G. L., Ocampo-Pérez, R., Moura, J. M., Cadaval Jr., T. R. S., and Pinto, L. A. A. (2016b). Adsorption rate of reactive black 5 on chitosan based materials: Geometry and swelling effects, *Adsorption*, **22**, 973–983.

Dotto, G. L., Sharma, S. K., and Pinto, L. A. A. (2015). Biosorption of organic dyes: Research opportunities and challenges, in: Sharma, S. K., Ed., *Green Chemistry for Dyes Removal from Waste Water: Research Trends and Applications,* Scrivener Publishing LLC, Beverly, pp. 295–329.

Dwyer, K., Hosseinian, F., and Rod, M. (2014). The market potential of grape waste alternatives, *J. Food Res.*, **3**, 91–106.

Franco, D. S. P., Tanabe, E. H., and Dotto, G. L. (2017). Continuous adsorption of a cationic dye on surface modified rice husk: Statistical optimization and dynamic models, *Chem. Eng. Commun.*, **204**, 625–634.

Freundlich, H. M. F. (1906). Uber die adsorption in lösungen, *J. Phys. Chem.*, **57**, 385–470.

Giles, C. H., MacEwan, T. H., Nakhwa, S. N., and Smith, D. (1960). Studies in adsorption part XI: A system of classification of solution adsorption isotherms and its use in diagnosis of adsorption mechanisms and in measurement of specific surface areas of solids, *J. Chem. Soc.*, **786**, 3973–3993.

Goertzen, S. L., Theriault, K., Oickle, A. M., Tarasuk, A. C., and Andreas, H. A. (2010). Standardization of the Boehm titration: Part I–CO2 expulsion and endpoint determination, *Carbon*, **48**, 1252–1261.

Goldstein, J. I., Newbury, D. E., Echil, P., Joy, D. C., Romig Jr., A. D., Lyman, C. E., Fiori, C., and Lifshin, E. (1992). *Scanning Electron Microscopy and X-Ray Microanalysis*, Plenum Press, New York.

Ho, Y. S., and McKay, G. (1998). A comparison of chemisorption kinetic models applied to pollutant removal on various sorbents, *Proc. Saf. Environ. Prot.*, **76**, 332–340.

Jeon, C. (2015). Adsorption behavior of silver ions from industrial wastewater onto immobilized crab shell beads, *J. Ind. Eng. Chem.*, **32**, 195–200.

Lagergren, S. (1898). About the theory of so–called adsorption of soluble substances, *Kung. Sven. Vetenskap. Hand.*, **24**, 1–39.

Langmuir, I. (1918). The adsorption of gases on plane surfaces of glass, mica and platinum, *J. Am. Chem. Soc.*, **40**, 1361–1403.

Liu, Y. (2009). Is the free energy change of adsorption correctly calculated? *J. Chem. Eng. Data*, **54**, 1981–1985.

Liu, Y., and Liu, Y. J. (2008). Biosorption isotherms, kinetics and thermodynamics, *Sep. Purif. Technol.*, **61**, 229–242.

Milonjic, S. K. (2007). A consideration of the correct calculation of thermodynamic parameters of adsorption, *J. Serbian Chem. Soc.*, **72**, 1363–1367.

Muñoz, A. J., Espínola, F., and Ruiz, E. (2017). Biosorption of Ag(I) from aqueous solutions by *Klebsiella* sp. 3S1, *J. Hazard. Mater.*, **329**, 166–177.

Park, J., and Regalbuto, J. R. (1995). A simple, accurate determination of oxide PZC and the strong buffering effect of oxide surfaces at incipient wetness, *J. Colloid Interface Sci.*, **175**, 239–252.

Sari, A., and Tüzen, M. (2013). Adsorption of silver from aqueous solution onto raw vermiculite and manganese oxide–modified vermiculite, *Micro. Meso. Mater.*, **170**, 155–163.

Saucier, C., Adebayo, M. A., Lima, E. C., Cataluña, R., Thue, P. S., Prola, L. D. T., Puchana-Rosero, M. J., Machado, F. M., Pavan, F. A., and Dotto, G. L. (2015). Microwave-assisted activated carbon from cocoa shell as adsorbent for removal of sodium diclofenac and nimesulide from aqueous effluents, *J. Hazard. Mater.*, **289**, 18–27.

Silverstein, R. M., Webster, F. X., and Kiemle, D. J. (2007). *Spectrometric Identification of Organic Compounds*, John Wiley & Sons, New York.

Sips, R. (1948). On the structure of a catalyst surface, *J. Chem. Phys.*, **16**, 490–495.

Song, X., Gunawan, P., Jiang, R., Leong, S. S. J., Wang, K., and Xu, R. (2011). Surface activated carbon nanospheres for fast adsorption of silver ions from aqueous solutions, *J. Hazard. Mater.*, **194**, 162–168.

Tappin, A. D., Barriada, J. L., Braungardt, C. B., Evans, E. H., Patey, M. D., Achterberg, E. P. (2010). Dissolved silver in European estuarine and coastal waters, *Water. Res.*, **44**, 4204–4216.

Torab-Mostaedi M., Asadollahzadeh M., Hemmati A., and Khosravi A. (2013). Equilibrium, kinetic, and thermodynamic studies for biosorption of cadmium and nickel on grapefruit peel, *J. Taiwan Inst. Chem. Eng.*, **44**, 294–301.

Vanni, G., Escudero, L. B., and Dotto, G. L. (2017). Powdered grape seeds (PGS) as an alternative biosorbent to remove pharmaceutical dyes from aqueous solutions, *Water Sci. Technol.*, **76**, 1177–1187.

Wajima, T. (2016). Synthesis of zeolitic material from green tuff stone cake and its adsorption properties of silver (I) from aqueous solution, *Micro. Meso. Mater.*, **233**, 154–162.

Wu, J. J., Lee, H. W., You, J. H., Kau, Y. C., and Liu, S. J. (2014). Adsorption of silver ions on polypyrrole embedded electrospun nanofibrous polyethersulfone membranes, *J. Colloid Interface Sci.*, **420**, 145–151.

Yedro, F. M., García–Serna, J., Cantero, D. A., Sobrón, F., and Cocero, M. J. (2015). Hydrothermal fractionation of grape seeds in subcritical water to produce oil extract, sugars and lignin, *Catalysis Today*, **257**, 160–168.

Zhang, M., Helleur, R., and Zhang, Y. (2015). Ion-imprinted chitosan gel beads for selective adsorption of Ag^{+} from aqueous solutions, *Carbohydr. Polym.*, **130**, 206–212.